An Improved Current-Sensorless Model Predictive Voltage Control for Four-Leg Voltage Source Inverters

Heng Guo
School of
Control Science and Engineering
Shandong University
Jinan, China
guoheng@mail.sdu.edu.cn

Yuxin Wei
School of
Control Science and Engineering
Shandong University
Jinan, China
202434888@mail.sdu.edu.cn

Mengmeng Jing
School of
Control Science and Engineering
Shandong University
Jinan, China
202014057@mail.sdu.edu.cn

Wenlong Ding
School of
Control Science and Engineering
Shandong University
Jinan, China
wlding@sdu.edu.cn

Bin Duan
School of
Control Science and Engineering
Shandong University
Jinan, China
duanbin@sdu.edu.cn

Chenghui Zhang*
School of
Control Science and Engineering
Shandong University
Jinan, China
zchui@sdu.edu.cn

***Abstract*—Four-leg voltage source inverters (VSIs) with LC output filter are commonly utilized to stabilize three-phase sinusoidal voltages under unbalanced loads conditions. However, conventional model predictive voltage control (MMPVC) for four-leg VSIs relies heavily on current sensors, leading to increased costs and suboptimal output voltage performance. To address these issues, this paper proposes an improved current-sensorless modulated model predictive voltage control (MMPVC) for four-leg VSIs to effectively reduce voltage tracking errors and total harmonic distortion (THDv). First, a readily implementable capacitor current extended state observer is constructed to replace current sensors and a corresponding discrete model is reconstructed. Then, four-vector MMPVC for four-leg VSIs is carefully designed. Especially, the ineffective voltage vectors are found, and their duration time is set as zero to optimize the output voltage performance in edge regions of sectors and over-modulation regions. Finally, experimental results validate the proposed approach, demonstrating substantial improvements in output voltage quality and tracking accuracy in over-modulation regions.**

***Index Terms*—model predictive voltage control, current-sensorless, four-leg voltage source inverters.**

I. Introduction

Three-phase four-leg voltage source inverters (VSIs) with LC output filter stand out as one of the best solutions to provide an ideal three-phase sinusoidal output voltage, even under severe unbalanced loads, thanks to high DC-link voltage utilization and flexible control of zero-sequence component [1], [2]. Therefore, it has been used in many independent power supply systems, including the distributed generation (DG) systems, uninterruptible power supply (UPS) systems, energy storage (ES) systems, and stand-alone AC applications systems [3].

Remarkably, model predictive voltage control (MPVC) is favorable for four-leg VSIs due to the merits of simplicity, fast dynamic response, and ability to handle multivariate constraints [4]. To reduce costs, many implementations replace physical current sensors with current estimators [5]–[8]. However, conventional MPVC suffers from degraded output voltage quality, leading to inaccuracy in current estimation and difficulty in voltage tracking.

To overcome these issues, researchers have proposed modulated model predictive voltage control (MMPVC), which employs multiple voltage vectors within a single cycle and incorporates modulation stages to improve output performance. In MMPVC, the duration time of each voltage vector is determined based on its cost function value [9]. Yet, MMPVC usually combines two voltage vectors or three voltage vectors in one sampling period [10]. While this approach generally enhances voltage quality compared to traditional MPVC, it typically combines only two or three voltage vectors per sampling period, limiting its effectiveness for four-leg VSIs. The additional zero-sequence component in four-leg VSIs demands the use of four voltage vectors for optimal performance. Based on this, in [11], four voltage vectors were selected in one cycle, and the performance in the over-modulation region is also optimized by removing the zero vector. The article realized high performance output voltage both in the linear region and in the over-modulation region, but exhibited poor tracking

This paper was supported by the National Key R&D Plan of China, Grant/AwardNumber: 2022YFF0712700, National Natural Science Foundation of China (No. 62203275, 62203265, 62133007, 62333013), Shandong Province Science Foundation (No. 2022HYYQ-022, ZR2022QF028, ZR2024QF101), Fellowship of China National Postdoctoral Program (No. BX20230209, 2024M751809).

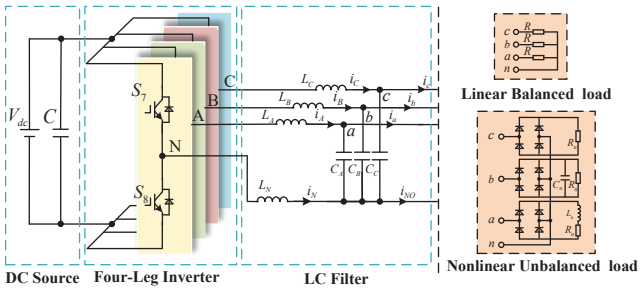

Fig. 1. Topology of four-leg VSI

performance.

To overcome these shortcomings, this paper proposed an improved current-sensorless MMPVC for four-leg VSIs. The key contributions are:

1) A capacitor current extended state observer is constructed to replace current sensors, enhancing estimation accuracy.
2) An improved MMPVC strategy is proposed to reduce voltage tracking errors and voltage total harmonic distortion (THDv), especially in edge regions of sectors and over-modulation regions.

The remaining parts of this article are arranged as follows. In Section II, the state variable is reconstructed as capacitor current, and the change in output current is used as an error for the extend state observer design. Based on this, a simple current-sensorless mathematical model is developed. In Section III, the four-vector MMPVC is briefly extended to four-leg VSIs, the duration time of ineffective voltage vectors are set to zero. In Section IV, the effectiveness of the proposed MMPVC strategy is verified by comparative experimental studies. Conclusions are drawn in section V.

II. SYSTEM DESCRIPTION

The topology of the four-leg VSI studied in this article is shown in Fig. 1, where V_{dc} is the DC-link voltage, L_a, L_b and L_c are three-phase filter inductor, i_{La}, i_{Lb}, i_{Lc} are three-phase inductor currents, i_{ca}, i_{cb}, i_{cc} are three-phase capacitive currents, i_{oa}, i_{ob}, i_{oc} are three-phase output currents, L_n is the zero-sequence inductor.

With the addition of the fourth leg, the coupling between the three phases is more severe. To better handle the coupling introduced by the fourth leg, the three-phase variables are transformed into the $\alpha\beta\gamma$ reference frame, enabling independent control of decoupled state variables [12]. The mathematical model in $\alpha\beta\gamma$ reference frame is described by equation (1).

$$\begin{cases} \dfrac{di_{Lx}}{dt} = \dfrac{1}{L_x}(v_{ix} - v_{cx}) \\ \dfrac{dv_{cx}}{dt} = \dfrac{1}{C_x}(i_{Lx} - i_{ox}) \end{cases} \tag{1}$$

where $x = \alpha,\ \beta,\ \gamma$, $L_{\alpha,\beta} = L$, $L_\gamma = 3L_n + L$, $C_{\alpha,\beta,\gamma} = C$. As can be seen from (1), the output current needs to be measured to observe the inductor current. If only the capacitor voltage is used, it is impossible to directly observe two currents at the same time. Therefore, the state variable is firstly converted from inductive current to capacitive current, as described in equation (2).

$$\begin{cases} \dfrac{di_{cx}}{dt} = \dfrac{di_{Lx}}{dt} - \dfrac{di_{ox}}{dt} = \dfrac{1}{L_x}(v_{ix} - v_{cx}) - \dfrac{di_{ox}}{dt} \\ \dfrac{dv_{cx}}{dt} = \dfrac{1}{C}(i_{Lx} - i_{ox}) = \dfrac{i_{cx}}{C} \end{cases} \tag{2}$$

To simplify the design of the observer, it is often assumed that change in output current is constant ($di_{ox}/dt = 0$). However, this approximation results in inaccurate current estimation and poor immunity. Therefore, denoting di_{ox}/dt as f_x, the capacitor current extended state observer can be designed as (3).

$$\begin{cases} \dfrac{d\hat{v}_{xn}}{dt} = \dfrac{1}{C}\hat{i}_{cx} + k_1(v_{cx} - \hat{v}_{cx}) \\ \dfrac{d\hat{i}_{cx}}{dt} = \dfrac{1}{L_x}(v_{ix} - \hat{v}_{cx}) - \hat{f}_x + k_2(v_{cx} - \hat{v}_{cx}) \\ \dfrac{d\hat{f}_x}{dt} = k_3(v_{cx} - \hat{v}_{cx}) \end{cases} \tag{3}$$

where the notation " $\wedge$ " represents the estimated value, while k_1, k_2 and k_3 are the estimator gains.

Furthermore, based on the forward Euler method, the discrete model of the proposed capacitor current extended state estimator is derived as

$$\begin{cases} \hat{v}_{cx}(k+1) = \hat{v}_{cx}(k) + T_s\left(\dfrac{1}{C_f}\hat{i}_{cx}(k) + k_1 e_x(k)\right) \\ \hat{i}_{cx}(k+1) = \hat{i}_{cx}(k) \\ \qquad\qquad + T_s\left(\dfrac{1}{L_x}(v_{ix}(k) - \hat{v}_{cx}(k)) - f_x(k) + k_2 e_x(k)\right) \\ \hat{f}_x(k+1) = \hat{f}_x(k) + T_s k_3 e_x(k) \end{cases} \tag{4}$$

where T_s is the sampling time, $e_x(k) = v_{cx}(k) - \hat{v}_{cx}(k)$.

The estimator gains k_1, k_2 and k_3 in (4) can be selected using the direct pole assignment strategy. Besides, the proposed capacitor current extend estimator is rewritten as follows:

$$\underbrace{\begin{bmatrix} \hat{V}_{Cx}(k+1) \\ \hat{i}_{c\alpha}(k+1) \\ \hat{F}(k+1) \end{bmatrix}}_{\hat{\mathbf{x}}(k+1)} = \underbrace{\begin{bmatrix} 1 & \frac{T_s}{C_f} & 0 \\ -\frac{T_s}{L_f} & 1 & T_s \\ 0 & 0 & 1 \end{bmatrix}}_{\mathbf{G}} \underbrace{\begin{bmatrix} \hat{v}_{f\alpha}(k) \\ \hat{i}_{c\alpha}(k) \\ \hat{F}(k) \end{bmatrix}}_{\mathbf{x}(k)} + \underbrace{\begin{bmatrix} 0 \\ \frac{T_s}{L_f} \\ 0 \end{bmatrix}}_{\mathbf{H}} v_{i\alpha}(k) + \underbrace{\begin{bmatrix} k_1 T_s & 0 & 0 \\ k_2 T_s & 0 & 0 \\ k_3 T_s & 0 & 0 \end{bmatrix}}_{\mathbf{K}} [\mathbf{x}(k) - \hat{\mathbf{x}}(k)] \tag{5}$$

Accordingly, the eigenpolynomial of (5) is expressed as

$$\begin{aligned} \det(z\mathbf{I} - \mathbf{G} + \mathbf{K}) = {} & z^3 + (k_1 T_s - 3)z^2 \\ & + \left(\frac{T_s^2}{CL_x} + 3 + \frac{T_s^2 k_2}{C} - 2T_s k_1\right)z \\ & - \frac{T_s}{C_f} - 1 - \frac{T_s^2 k_2}{C} + \frac{T_s^3 k_3}{C} + T_s k_1 \end{aligned} \tag{6}$$

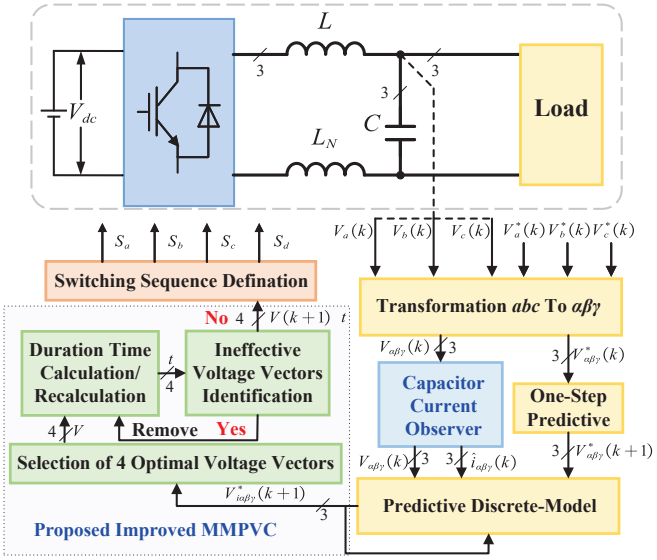

Fig. 2. Control block diagram of the proposed method.

where I is the three-dimensional unit matrix. To make the roots of the characteristic equation both fall at $-\omega_0$, k_1, k_2 and k_3 can be obtained by

$$\det\left(z\mathbf{I}-\mathbf{G}+\mathbf{K}\right)=\left(z-\left(1-\omega_0 T_s\right)\right)^2 \tag{7}$$

By comparing the coefficients of (7), the estimator gains k_1, k_2 and k_3 can be obtained as

$$\begin{cases} k_1 = 3\omega_0 \\ k_2 = 3C_x\omega_0^2 - \dfrac{1}{L_x} \\ k_3 = C_x\omega_0^3 \end{cases} \tag{8}$$

Based on deadbeat control proposed in [12], voltage reference can be obtained by

$$\begin{aligned} u_{ix}(ref) =& \frac{L_x}{T_s}\left(\frac{C}{T_s}\left(v_{cx}(ref)-v_{cx}(k)\right)-\hat{i}_{cx}(k)\right)+\hat{f}_x(k)) \\ &+ v_{cx}(ref) \end{aligned} \tag{9}$$

where i_{cx} and f are replaced by $\hat{i}_{cx}$ and $\hat{f}$ because they can not be directly measured. where $v_{cx}(ref)$ is the voltage reference and it is synthesized by proposed MMPVC to generate the final gating pulses in this article.

III. PROPOSED IMPROVED MMPVC FOR FOUR-LEG VSIS

The control block diagram of the proposed method is shown in Fig. 2. Fig. 3 shows voltage vectors of four-leg VSIs in 3-D space. To obtain the optimal voltage vectors, all basic voltage vectors are evaluated by the cost function for voltage tracking [11].

$$g(v)=\sqrt{\sum_{x=\alpha,\beta,\gamma}\left(v_x(ref)-v_x\right)^2} \tag{10}$$

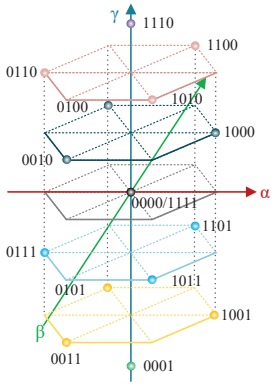

Fig. 3. Voltage vectors of four-leg VSIs in 3-D space.

Then, the optimal four voltage vectors are applied in one cycle (recorded as u_0, u_1, u_2 and u_3), and their duration time is usually calculated by (11) [9]. However, equation (11) inaccurately calculates the duration time of voltage vectors, resulting in low voltage tracking accuracy in the edge regions of sectors and the overmodulation regions. Specifically, in these regions, the duration time of some voltage vectors should be close to zero, but the results calculated using equation (11) are contrary. Therefore, in the proposed method, such voltage vectors are recognized as ineffective voltage vectors, and their duration time is set to zero and reallocated to the remaining voltage vectors.

$$\begin{cases} t_{1,u0} = \dfrac{G_{u2}G_{u3}G_{u4}}{G_u}T_s \\ t_{1,u1} = \dfrac{G_{u1}G_{u3}G_{u4}}{G_u}T_s \\ t_{1,u2} = \dfrac{G_{u1}G_{u2}G_{u4}}{G_u}T_s \\ t_{1,u3} = \dfrac{G_{u1}G_{u2}G_{u3}}{G_u}T_s \end{cases} \tag{11}$$

where T_s is the duration time of one cycle, $G_u = G_{u1}G_{u2}G_{u3} + G_{u1}G_{u2}G_{u4} + G_{u1}G_{u2}G_{u4} + G_{u2}G_{u3}G_{u4}$.

The simplified execution steps of the proposed MMPVC are shown below:

Step 1: Based on (4) and (9), the capacitor current is estimated, and the reference voltage can be calculated.

Step 2: According to the location of the reference voltage, four candidate voltage vectors are preselected, and their duration time is calculated by (11).

Step 3: Among all candidate voltage vectors, the duration time of the voltage vector with the largest cost function value is set to zero. Assuming that the duration time of u_3 is set to zero, the duration time of the remaining vector is allocated according to (12).

Step 4: If the remaining voltage vectors synthesize the reference voltage vector more accurately, u_3 is identified as an ineffective voltage vector. Step 3 is repeated to further determine whether there are still ineffective voltage vectors. If not, it indicates no ineffective vector among the candidate voltage vectors. Then, four voltage vectors and their reallocated time is fed into the modulator.

$$\begin{cases} t'_{u0} = t_{u0} * t_{u3} \frac{t_{u0}}{T_s} \\ t'_{u1} = t_{u1} * t_{u3} \frac{t_{u1}}{T_s} \\ t'_{u2} = t_{u2} * t_{u3} \frac{t_{u2}}{T_s} \end{cases} \tag{12}$$

Compared with traditional methods, this approach can eliminate ineffective voltage vectors, and improve tracking accuracy in overmodulation regions.

IV. EXPERIMENTAL RESULTS

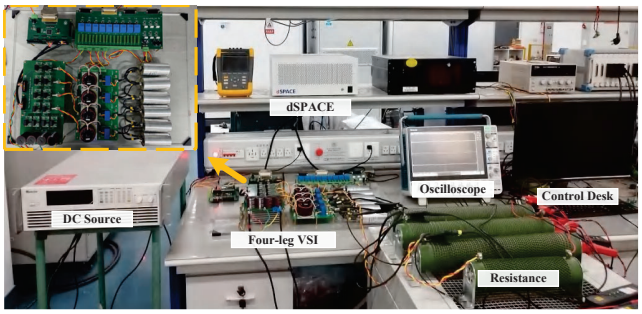

Fig. 4. Experimental setup for verification of the proposed scheme.

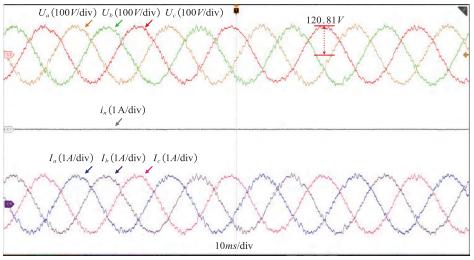

(a)

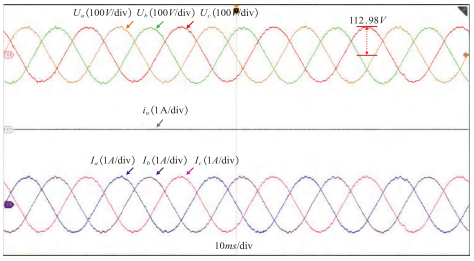

(b)

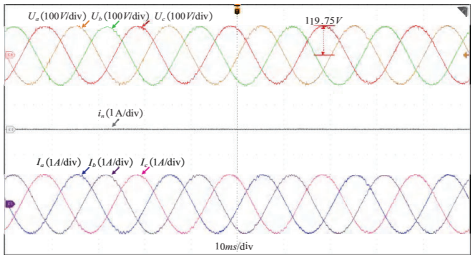

(c)

Fig. 5. Voltage and current waveforms in the linear region. (a) MPVC. (b) Four-vector MMPVC. (c) Proposed MMPVC.

TABLE I
GENERAL PARAMETERS OF THE IMPLEMENTED SYSTEMS

Parameter	Symbol	Value
Input Voltage	V_{dc}	$240V/200V$
Filter Capacitor	C_A, C_B,C_C	$60\mu F$
Filter Inductor	L_A, L_B, L_C, L_N	$1.5mH$
Resistive load	R_a,R_b,R_c	10Ω

In order to verify the effectiveness and superiority of the proposed MMPVC, an experimental platform of the four-leg VSI was established, as shown in Fig. 4. The main parameters are listed in Table I. The FS-MPVC [4], four-vector MMPVC and proposed MMPVC are implemented on a dSPACE DS2004 board. The experiment comprises the following two cases:

1) **In the linear region**, Fig. 5 shows the voltage waveforms and current waveforms of three methods under the condition that the peak of phase reference voltage at 120V and DC-link voltage at 240V. The comparison results of THDv and tracking error are recorded in Table II.
2) **In the overmodulation region**, Fig. 6 shows the voltage and current waveforms of the three methods under the condition that the peak of the phase reference voltage at 120V and the DC-link voltage at 200V. The comparison results of THDv and tracking error are recorded in Table III.

TABLE II
COMPARISON RESULTS OF THDV AND TRACKING ERROR IN THE LINEAR REGION.

Method	THDv	Tracking error
FS-MPVC	7.46%	0.81V
Four-Vector MMPVC	2.22%	7.02V
Proposed MMPVC	2.18%	0.25V

Form the experimental results, the following conclusions can be drawn:

1) All three methods can effectively track the three-phase voltage reference, both in the linear region and in the over-modulation region. Among them, MPVC and the proposed method have better tracking performance than the four-vector MMPVC.
2) While the four-vector MMPVC can demonstrate improved output THDv in the linear region region, it works

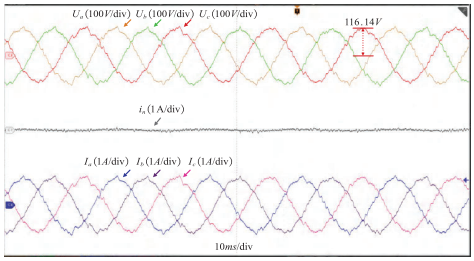

(a)

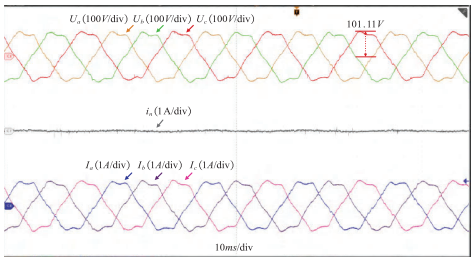

(b)

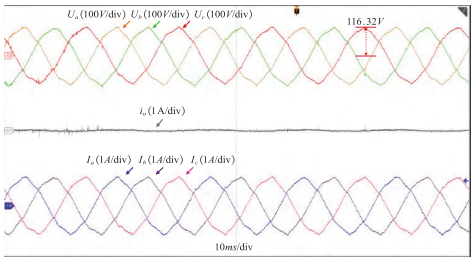

(c)

Fig. 6. Voltage and current waveforms in the overmodulation region. (a) MPVC. (b) Four-vector MMPVC. (c) Proposed MMPVC.

TABLE III
COMPARISON RESULTS OF THDV AND TRACKING ERROR IN THE OVER-MODULATION REGION.

Method	THDv	Tracking error
FS-MPVC	5.38%	3.86V
Four-Vector MMPVC	8.35%	18.89V
Proposed MMPVC	4.18%	3.68V

very poorly in the over-modulation region, which is attributed to the difficulty in maintaining the output voltage. Whereas, MPVC exhibits poor output THDv performance both in the linear region and in the over-modulation region, which is higher than the proposed method.

In summary, the experimental results show that although all three methods can track the reference voltage, but the proposed MMPVC achieves better output voltage performance and tracking capability.

V. CONCLUSIONS

This paper proposes a novel current-sensorless MMPVC strategy for four-leg VSIs with LC output filter. By replacing current sensors with a capacitor current extended state observer and optimizing the duration time of voltage vectors, the proposed method significantly enhances voltage tracking accuracy and reduces THDv. Experimental results verified its superiority over conventional methods in both linear and over-modulation regions, highlighting its potential for high-performance and cost-effective power conversion.

REFERENCES

[1] R Zhang, VH Prasad, D Boroyevich, and FC Lee. Three-dimensional space vector modulation for four-leg voltage-source converters. *IEEE TRANSACTIONS ON POWER ELECTRONICS*, 17(3):314–326, MAY 2002.

[2] Roberto Cardenas, Carlos Juri, Ruben Pena, Patrick Wheeler, and Jon Clare. The application of resonant controllers to four-leg matrix converters feeding unbalanced or nonlinear loads. *IEEE TRANSACTIONS ON POWER ELECTRONICS*, 27(3):1120–1129, MAR 2012.

[3] Joan Rocabert, Alvaro Luna, Frede Blaabjerg, and Pedro Rodriguez. Control of power converters in ac microgrids. *IEEE TRANSACTIONS ON POWER ELECTRONICS*, 27(11, SI):4734–4749, NOV 2012.

[4] Changming Zheng, Tomislav Dragicevic, and Frede Blaabjerg. Current-sensorless finite-set model predictive control for LC-filtered voltage source inverters. *IEEE TRANSACTIONS ON POWER ELECTRONICS*, 35(1):1086–1095, JAN 2020.

[5] Sebastian Gomez Jorge, Jorge A. Solsona, and Claudio A. Busada. Control scheme for a single-phase grid-tied voltage source converter with reduced number of sensors. *IEEE TRANSACTIONS ON POWER ELECTRONICS*, 29(7):3758–3765, JUL 2014.

[6] Yasser Abdel-Rady Ibrahim Mohamed, Ehab F. El-Saadany, and Magdy M. A. Salama. Adaptive grid-voltage sensorless control scheme for inverter-based distributed generation. *IEEE TRANSACTIONS ON ENERGY CONVERSION*, 24(3):683–694, SEP 2009.

[7] Yasser Abdel-Rady I. Mohamed, M. A. Rahman, and R. Seethapathy. Robust line-voltage sensorless control and synchronization of LCL-filtered distributed generation inverters for high power quality grid connection. *IEEE TRANSACTIONS ON POWER ELECTRONICS*, 27(1), JAN 2012.

[8] Roberto A. Fantino, Claudio A. Busada, and Jorge A. Solsona. Observer-based grid-voltage sensorless synchronization and control of a VSI-LCL tied to an unbalanced grid. *IEEE TRANSACTIONS ON INDUSTRIAL ELECTRONICS*, 66(7):4972–4981, JUL 2019.

[9] Leilei Guo, Mo Chen, Yanyan Li, Pengshuai Wang, Nan Jin, and Jie Wu. Hybrid multi-vector modulated model predictive control strategy for voltage source inverters based on a new visualization analysis method. *IEEE TRANSACTIONS ON TRANSPORTATION ELECTRIFICATION*, 9(1):8–21, MAR 2023.

[10] Tong Liu, Alian Chen, Wei Wang, Xi Liu, Qicai Ren, Guanguan Zhang, and Chenghui Zhang. An improved model predictive control to enhance voltage performance for LC filtered three-level inverters with voltage feedback only. *IEEE TRANSACTIONS ON INDUSTRIAL INFORMATICS*, 19(9):9809–9820, SEP 2023.

[11] Dan Xiao, Kazi Saiful Alam, and Muhammed Fazlur Rahman. Predictive duty cycle control for four-leg inverters with LC output filter. *IEEE TRANSACTIONS ON INDUSTRIAL ELECTRONICS*, 68(5):4259–4268, MAY 2021.

[12] Mohammad Pichan, Hasan Rastegar, and Mohammad Monfared. Deadbeat control of the stand-alone four-leg inverter considering the effect of the neutral line inductor. *IEEE TRANSACTIONS ON INDUSTRIAL ELECTRONICS*, 64(4):2592–2601, APR 2017.